LOCAL SPECIFIC BENDING STIFFNESS IDENTIFICATION OF AN UNHOMOGENEOUS COMPOSITE PLATE VIA HIGH-RESOLUTION WAVEVECTOR ANALYSIS

Pierre Margerit, Arthur Lebée, and Jean-François Caron

Laboratoire Navier, UMR 8205, École des Ponts, IFSTTAR, CNRS, UPE, Champs-sur-Marne, France

Abstract

An original Non Destructive Evaluation procedure is presented. It allows the *in-situ* identification of the local elastic behavior of a composite plate, with a little sensitivity to boundary conditions and loads. The harmonic response of a of a composite plate is approximated as a combination of plane waves. By the application of a high resolution wavevector analysis tool (HRWA), the wavevectors of these waves can be extracted. While theoretical wavevectors can be derived from plate's local equations of motions, an inverse identification problem can be formulated. Here, the Classical Lamination Plate Theory is used in order to identify the local specific bending stiffness of a composite CFRP plate with spatially varying fiber orientations. Experimentally identified plate properties are in good agreement with the predictions computed from material properties.

1 Introduction

Composite materials are difficult to characterize, because of their complex behavior. Indeed, a number of parameters such as the anisotropy, the stacking sequence or the heterogeneity of the mechanical properties influence the global behavior of the final composite structure. In addition, emerging technologies like *Automated Fibre Placement* [1, 2] allows to make composite parts with *spatially varying* fiber orientations. First, characterization methods based on modal data [3, 4, 5, 6] are suited for the identification of structural properties in low frequencies. However, a good estimation is hard to achieve when the structural damping is strong and/or the boundary conditions not well controlled. Second, a number of methods based on ultrasonic data [7] can be used. Local mechanical properties can be estimated. Recently, the development of full-field measurement methods [8, 9] helped the development of *medium frequency* methods [10, 11, 12]. The aim is to use the large amount of experimental data given by these measurement techniques to fill the gap between low and high frequency methods.

In this work, an original identification procedure of composite plate behavior is developed, suited for *in-situ* applications. It is applied of full-field data measured on regular grids. It focuses on the extraction of plane wave in the steady harmonic regime. From the extracted wavevectors ans the Classical Lamination Theory is formulated a linear inverse identification problem. At the end, the local generalized specific bending stiffness tensor of an anisotropic plate with heterogeneous properties can be identified.

The paper is organized as follows : First, the dispersion equations of a thin anisotropic laminated plate are derived from the Classical Lamination Theory, giving the relation between the plane wave's wavevectors, the frequency and the generalized plate mechanical properties. Second, the principle of the High Resolution Wavevector Analysis, which is used to extract the wavevectors from the measurements, is presented. Third, the inverse identification problem, based on the extracted wavevectors, is developed. Finally, an experimental application is shown. The generalized bending behavior of a plate with piece-wise constant mechanical properties is locally identified and compared to predictions.

2 Principle of the method

2.1 Bending waves travelling in a thin anisotropic plate

The dynamical behavior of a thin laminated plate in low frequencies can be well described by the Classical Lamination Theory (CLT), as the ratio of the wavelength over the plate thickness is low. More precisely, when the plate possesses a mirror symmetry in regard to its neutral plane, the equation governing the bending motion is expressed as a fourth-order differential operator on the transverse displacement U_3 only :

$$\Big(\mathrm{D}_{11}\frac{\partial}{\partial x_1^4}+\mathrm{D}_{22}\frac{\partial}{\partial x_2^4}+2(\mathrm{D}_{12}+2\mathrm{D}_{66})\frac{\partial}{\partial x_1^2\partial x_2^2}+4\mathrm{D}_{16}\frac{\partial}{\partial x_1^3\partial x_2}+4\mathrm{D}_{26}\frac{\partial}{\partial x_1\partial x_2^3}+\mathrm{M}\frac{\partial}{\partial t^2}\Big)U_3(\boldsymbol{x}) = f_3(\boldsymbol{x}) \quad (1)$$

with $\boldsymbol{x} = (x_1, x_2)$. The generalized parameters $\mathrm{D}_{\alpha\beta}$ and M respectively take into account the stiffness and mass distribution over the plate thickness h :

$$\mathrm{D}_{\alpha\beta} = \int_{-h/2}^{h/2} x_3^2 C_{\alpha\beta}(x_3)\,\mathrm{d}x_3 \quad , \quad \mathrm{M} = \int_{-h/2}^{h/2} \rho(x_3)\,\mathrm{d}x_3 \qquad (2)$$

When considering a zone of the plate free of load, the 2D space and time variable separation approach can be used in order to compute plane wave solutions that takes the following form :

$$U_3(\boldsymbol{x}, t) = U\,\mathrm{e}^{i(\omega t-\boldsymbol{k}\cdot\boldsymbol{x})} \qquad (3)$$

where ω is the frequency and $\boldsymbol{k}$ the complex wavevector :

$$\boldsymbol{k} = \boldsymbol{\kappa} + i\boldsymbol{\tau} = \begin{bmatrix} k_1 \\ k_2 \end{bmatrix} = \|\boldsymbol{\kappa}\| \begin{bmatrix} \cos\phi \\ \sin\phi \end{bmatrix} + i\,\|\boldsymbol{\tau}\| \begin{bmatrix} \cos\psi \\ \sin\psi \end{bmatrix} \qquad (4)$$

$\boldsymbol{\kappa}$ and $\boldsymbol{\tau}$ respectively denote the oriented spatial frequency and decay of the wave. In the general case they are not colinear ($\phi \neq \psi$). Combining (Eq. 3) and (Eq. 1) leads to the dispersion equation, describing the complex wavevector components (k_1, k_2) as a function of the frequency ω :

$$k_1^4\mathrm{D}_{11} + k_2^4\mathrm{D}_{22} + 2k_1^2k_2^2(\mathrm{D}_{12} + 2\mathrm{D}_{66}) + 4k_1^3k_2\mathrm{D}_{16} + 4k_1k_2^3\mathrm{D}_{26} - \omega^2\mathrm{M} = 0 \qquad (5)$$

For equal and fixed $\phi = \psi$, the complex wavenumber $k = \|\boldsymbol{\kappa}\| + i\,\|\boldsymbol{\tau}\|$ is solution of the following fourth root :

$$k^4 = \omega^2\Big(\frac{c^4\mathrm{D}_{11} + s^4\mathrm{D}_{22} + 2c^2s^2(\mathrm{D}_{12} + 2\mathrm{D}_{66}) + 4c^3s\mathrm{D}_{16} + 4cs^3\mathrm{D}_{26}}{\mathrm{M}}\Big)^{-1} \qquad (6)$$

with $c = \cos\phi$ and $s = \sin\phi$. This equation has four distinct solutions : two real and two imaginary. These two types of solution are respectively related to *propagating* waves which support lays on the entire plate, and *evanescent* waves which spatial decay is strong and account for boundary conditions mostly. When the medium is viscoelastic, it can be modeled by complex stiffness components $\mathrm{D}_{\alpha\beta}$ which can depend on frequency. Consequently the wavevector solutions are not purely real or imaginary any more, but become complex. Hence a *spatial decay ratio* γ can be defined :

$$\gamma = \frac{\|\boldsymbol{\tau}\|}{\|\boldsymbol{\kappa}\|} \qquad (7)$$

From the value of γ can be sorted two types of waves : *mostly propagating* ($\gamma < 1$) and *mostly evanescent* ($\gamma > 1$). Focusing on the propagating waves, the imaginary part $\boldsymbol{\tau}$ of the wavevector is neglected in the present work. Consequently the equation (Eq. 6) can be rewritten in order to rise a frequency invariant b dependent on the wave propagation angle ϕ only :

$$b(\phi) = \frac{\omega^2}{||\boldsymbol{\kappa}||^4} = \frac{c^4 \mathrm{D}_{11} + s^4 \mathrm{D}_{22} + 2c^2 s^2 (\mathrm{D}_{12} + 2\mathrm{D}_{66}) + 4c^3 s \mathrm{D}_{16} + 4cs^3 \mathrm{D}_{26}}{\mathrm{M}} \tag{8}$$

where $b(\phi)$ can be interpreted as the equivalent specific bending stiffness of the plate in the direction ϕ. It is linearly dependent on the components of the *specific bending stiffness tensor* **B**, which are given as :

$$\mathrm{B}_{\alpha\beta} = \frac{\mathrm{D}_{\alpha\beta}}{\mathrm{M}} \tag{9}$$

For composite plates with mechanical properties varying *slowly* in space (relatively to the wavelength $\lambda = 2\pi/||\boldsymbol{\kappa}||$), dispersion equations can still be formulated, but with *local* parameters $\mathrm{D}_{\alpha\beta}(\boldsymbol{x})$ and $\mathrm{M}(\boldsymbol{x})$. In consequence, the local bending stiffness components $\mathrm{B}_{\alpha\beta}(\boldsymbol{x})$ can be identified from some locally extracted wavevectors. It has to be noticed that no attention has been given to the boundary conditions and loads applied to the plate. Indeed, the preceding developments apply on free zones of the plate, that has to be located far enough from singularities. However, it has been observed that the impact of these singularities in the wavevector identification is mostly contained in the imaginary part $\boldsymbol{\tau}$, thus having a little effect on the identification of **B**.

With a method suited to extract the local wavevectors of bending waves travelling in an anisotropic plate in the steady harmonic regime, one is consequently able to identify the local specific bending stiffness tensor components. The proposed work uses the High Resolution Wavevector Analysis to extract these wavevectors from a measured plate response.

2.2 The High Resolution Wavevector Analysis

The High Resolution Wavevector Analysis (HRWA) has been recently developed by the authors as a tool for the characterization of anisotropic plates. It makes use of the ESPRIT algorithm [13], originally developed for telecommunication applications. A two-dimensional version of the algorithm [14] is used here. As it is not the main focus of the present work, not much details are given about the theoretical background and implementation of the HRWA. Basically, the ESPRIT algorithm aims at estimating the $2 \times R$ complex parameters $(u_r, \boldsymbol{k}_r)$ of a signal model $s(\boldsymbol{x})$ composed of a sum of R decaying exponential embedded in an additive noise $n(\boldsymbol{x})$:

$$s(\boldsymbol{x}) = \sum_r^R u_r \, \mathrm{e}^{i \boldsymbol{k}_r \cdot \boldsymbol{x}} + n(\boldsymbol{x}) \tag{10}$$

The algorithm makes use of the so-called *rotational invariance* of this signal to estimate the parameters. In the counterpart, the signal has to be measured over a regular spatial grid mesh $\boldsymbol{X}$ of steps Δ_1 and Δ_2 and size $L_1 \times L_2$:

$$X_{nm} = \boldsymbol{x}_0 + n\Delta_1 \boldsymbol{e}_1 + m\Delta_2 \boldsymbol{e}_2 \tag{11}$$

The order of the signal R is estimated thanks to the ESTER criterion [15] in its two-dimensional version [16]. The HRWA consists in applying the ESPRIT algorithm on steady harmonic plate responses $s(\boldsymbol{X}, \omega)$ measured over a frequency range. It can be summarized as follows :

1. Measure the response of the plate $s(\boldsymbol{X}, t)$ to a load that can be transient or stationary and over a regular grid $\boldsymbol{X}$ (Eq. 11)
2. Take the time Fourier transform of the plate response $\mathrm{TF}\{s(\boldsymbol{X}, t)\} = s(\boldsymbol{X}, \omega)$

3. For each frequency ω_i, apply the ESPRIT algorithm to $s(\boldsymbol{X}, \omega)$ in order to extract a number of complex wavevectors $\boldsymbol{k}$

At the end, one obtains a collection of wavevectors as a function of the frequency.

An additional step consists in taking only the most propagating extracted waves into account. Indeed, the identification of evanescent waves is more sensitive to applied boundary conditions and noise than the identification of propagating waves. In order to delete these extracted evanescent waves, one can fix a threshold $\gamma_{\max}$ in the maximum spatial decay γ_r computed with (Eq. 7). At the end, only extracted wavevectors fulfilling the following criterion are kept :

$$\gamma_r < \gamma_{\max} \tag{12}$$

2.3 Inverse identification of the specific bending stiffness

As the equation (Eq. 8) linearly depends on the specific bending stiffness components $\mathrm{B}_{\alpha\beta}$, a linear system can be built with the P extracted frequency-wavevector pairs $(\omega_p, \boldsymbol{\kappa}_p)$ as data and the $\mathrm{B}_{\alpha\beta}$ as unknowns :

$$\mathbf{A}\, \boldsymbol{y} = \boldsymbol{b} \tag{13}$$

with

$$\mathbf{A} = \begin{bmatrix} \boldsymbol{a}_1 & \cdots & \boldsymbol{a}_P \end{bmatrix}^{\mathsf{T}} \tag{14}$$

$$\boldsymbol{a}_p = \begin{bmatrix} c_p^4 & s_p^4 & 2c_p^2 s_p^2 & 4c_p^3 s_p & 4c_p s_p^3 \end{bmatrix} \tag{15}$$

$$y = \begin{bmatrix} \mathrm{B}_{11} & \mathrm{B}_{22} & \mathrm{B}_{12} + 2\mathrm{B}_{66} & \mathrm{B}_{16} & \mathrm{B}_{26} \end{bmatrix} \tag{16}$$

$$b = \begin{bmatrix} \frac{\omega_1^2}{\|\boldsymbol{\kappa}_1\|^4} & \cdots & \frac{\omega_P^2}{\|\boldsymbol{\kappa}_P\|^4} \end{bmatrix}^{\mathsf{T}} \tag{17}$$

As a consequence, the $\mathrm{B}_{\alpha\beta}$ can be estimated by direct linear fitting methods like Least-Squares, Total Least-Squares or Weighted Least-Squares. In the proposed work, the Least-Square estimation is used :

$$\boldsymbol{y} = \left(\mathbf{A}^{\mathsf{H}} \mathbf{A}\right)^{-1} \mathbf{A}^{\mathsf{H}} \boldsymbol{b} \tag{18}$$

3 Application to an unhomogeneous CFRP laminated plate

3.1 The experimental setup

For the need of the study, a square symmetric laminated CFRP plate of 30 cm width has been fabricated. It is made with carbon prepreg layers (150 g/m^2). The stacking sequence is $[\theta, 90°]_{\mathrm{S}}$, with a spatially varying θ. In practice, θ is made piece-wise constant by superimposing square patches with different fiber orientations over the two homogeneous central layers at 90°, which are continued along the entire plate. A top view picture of the plate is shown in (Fig. 1a). The 36 patches are made visible with the top layer fiber directions θ denoted as thin white lines. The plate is supported by silicon blocks at three of its corners. On the last corner, an electrodynamic shaker is fixed. It is used to apply a transverse load, with a stationary white noise as excitation signal. The excitation signal is band-pass filtered in order to excite only the frequencies contained in the range between 500 Hz and 22 kHz. The plate response is measured with a Scanning Laser Doppler Vibrometer (SLDV) over a regular grid of 100×100 points. At each point, 100 measurements of 0.1 seconds each are performed. After the computation of the transfer function estimator *H1* between the measured plate velocity and the electrical excitation signal, the average is computed over all the realizations. At the end, 2150 steady harmonic plate responses $s(\boldsymbol{X}, \omega_i)$, $i \in [\![1, 2150]\!]$ are obtained in the frequency range of interest.

E_L	E_T	G_{LT}	ν_{LT}	ρ	e
120 GPa	6.5 GPa	3.5 GPa	0.35	1300 kg/m^3	150 μm

TABLE 1: Material properties of the Carbon prepreg used to fabricate the laminated plate sample.

(a)

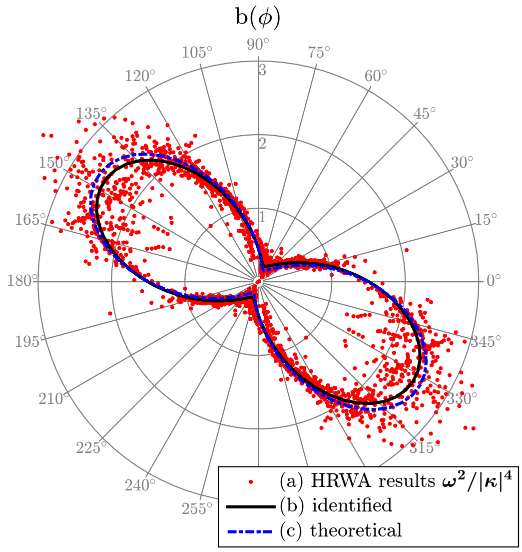

(b)

FIGURE 1: Identification of the local specific bending stiffness from HRWA results. (a) Top view of the plate (stacking sequence : $[\theta, 90°]_S$), which shows the fiber directions θ of the top carbon layer. (b) Local specific bending stiffness $b(\phi)$ (Eq. 8), identified on the location surrounded in red in (Fig. 1a) : HRWA results as red dot markers; black line : least-Square fit of (Eq. 18); blue line : indicative theoretical diagram from material engineering constants of (Table 1).

3.2 Application of the HRWA

The HRWA is performed on each of the steady harmonic plate responses that have been obtained, and at each zone corresponding to each patch location. As a consequence, the locally extracted wavevectors correspond to plate zones where the mechanical properties are constant. In order to avoid spurious wavevectors, the wavevector selection strategy (Eq. 12) is used, with $\gamma_{max} = 10\%$. At the end, one obtains a collection of approximately five thousand wavevectors by patch location.

3.3 Identification of the specific bending stiffness tensor components

For each patch location, the extracted wavevectors are used as data in the inverse problem (Eqs. 13 to 17). The procedure is illustrated in (Fig. 1b), for the patch surrounded by a red line in the plate picture (Fig. 1a). Firstly, the values of $b(\phi)$ computed from wavevectors (Eq. 8) are denoted as red dots. Secondly, the fitted model resulting of the inverse problem of (Eq. 18) is shown as a black line. Finally, the theoretical model is shown as a blue line. This prediction is computed from theoretical values of $D_{\alpha\beta}$ and M, derived from the approximate mechanical properties of the carbon prepreg, that are listed in (Table 1). The overall procedure is reproduced at each patch location. At the end, the specific bending stiffness tensor components $B_{\alpha\beta}$ are identified at each patch location. Both identified values, theoretical values and relative errors are shown in the (Fig. 2). Experimental and predicted values are in very good

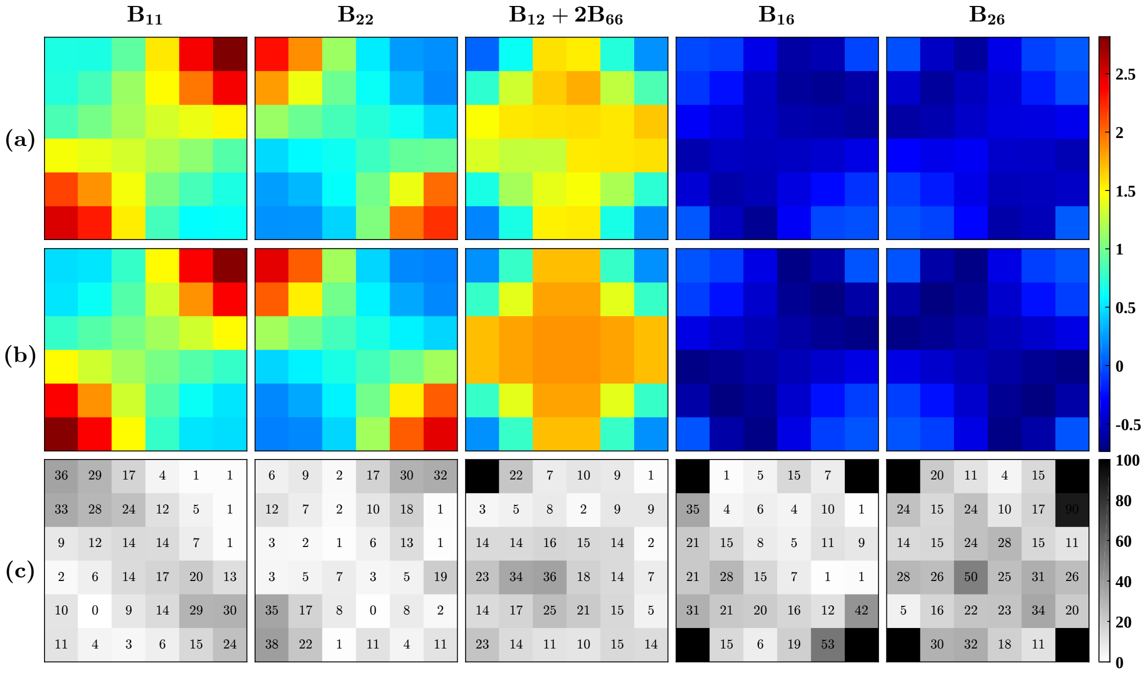

Figure 2: Components of the local specific bending stiffness tensor $\boldsymbol{B}$, for each patch of the plate, see (Fig. 1a). (a) Identified values from HRWA results ; (b) theoretical predictions from material properties in (Table 1) ; (c) rounded relative errors (%), black is more than 100%.

agreement. However, it can be observed that the coupling components B_{16} and B_{26} are weak, thus more difficult to identify.

4 Conclusion

A Non Destructive Evaluation method has been presented. Based on the extraction of plane waves in the full-field measurement of the steady harmonic response of a composite plate, it allows for the identification of the generalized bending properties. The plate anisotropy can be characterized, as well as the variation of the mechanical properties along the plate dimensions, with a little sensitivity to boundary conditions.

An experimental application has been presented on a laminated CFRP plate withe piece-wise constant mechanical properties. The experimental identified local plate properties are in good agreement with the theoretical values predicted from the approximate material properties.

Acknowledgments

This works is founded by the french National Research Agency (ANR), in the frame of the MAESSTRO project (*Modélisation Acoustique et Synthèse Sonore pour Tables d'haRmonie de pianOs*, ANR-14-CE07-0014).

Références

[1] Dirk H.J.A. Lukaszewicz, Carwyn Ward, and Kevin D Potter. The engineering aspects of automated prepreg layup : History, present and future. *Composites Part B : Engineering*, 43(3) :997–1009, 2012.

[2] P. Ribeiro, H. Akhavan, a. Teter, and J. Warmi ski. A review on the mechanical behaviour of curvilinear fibre composite laminated panels. *Journal of Composite Materials*, 48(22) :2761–2777, 2013.

[3] Jean-Marie Berthelot and Youssef Sefrani. Damping analysis of unidirectional glass and Kevlar fibre composites. *Composites Science and Technology*, 64(9) :1261–1278, 2004.

[4] Marc Rébillat and Xavier Boutillon. Measurement of relevant elastic and damping material properties in sandwich thick plates. *Journal of Sound and Vibration*, 330(25) :6098–6121, 2011.

[5] Marco Matter, Thomas Gmür, Joël Cugnoni, and Alain Schorderet. Identification of the elastic and damping properties in sandwich structures with a low core-to-skin stiffness ratio. *Composite Structures*, 93(2) :331–341, 2011.

[6] Romain Viala, Vincent Placet, and Scott Cogan. Identification of the anisotropic elastic and damping properties of complex shape composite parts using an inverse method based on finite element model updating and 3D velocity fields measurements (FEMU-3DVF) : Application to bio-base. *Composites Part A*, 106 :91–103, 2018.

[7] Mathias Kersemans, Ives De Baere, Joris Degrieck, Koen Van Den Abeele, Lincy Pyl, Filip Zastavnik, Hugo Sol, and Wim Van Paepegem. Nondestructive damage assessment in fiber reinforced composites with the pulsed ultrasonic polar scan. *Polymer Testing*, 34 :85–96, 2014.

[8] Christopher Niezrecki, Peter Avitabile, Christopher Warren, Pawan Pingle, and Mark Helfrick. A review of digital image correlation applied to structural dynamics. *AIP Conference Proceedings*, 1253(2010) :219–232, 2010.

[9] S J Rothberg, M S Allen, P Castellini, D Di Maio, J J J Dirckx, D J Ewins, B J Halkon, P Muyshondt, N Paone, T Ryan, H Steger, E P Tomasini, S Vanlanduit, and J F Vignola. An international review of laser Doppler vibrometry : Making light work of vibration measurement. *Optics and Lasers in Engineering*, 99(October 2016) :11–22, 2017.

[10] M. N. Ichchou, O. Bareille, and J. Berthaut. Identification of effective sandwich structural properties via an inverse wave approach. *Engineering Structures*, 30(10) :2591–2604, 2008.

[11] Frédéric Ablitzer, Charles Pézerat, Jean-Michel Génevaux, and Jérôme Bégué. Identification of stiffness and damping properties of plates by using the local equation of motion. *Journal of Sound and Vibration*, 333(9) :2454–2468, 2014.

[12] Raef Cherif, Jean Daniel Chazot, and Noureddine Atalla. Damping loss factor estimation of two-dimensional orthotropic structures from a displacement field measurement. *Journal of Sound and Vibration*, 356 :61–71, 2015.

[13] Richard Roy, A Paulraj, and Thomas Kailath. Estimation of signal parameters via rotational invariance techniques-ESPRIT. *IEEE Transactions on Acoustics, Speech and Signal Processing*, 37(7) :94–101, 1989.

[14] Stéphanie Rouquette and Mohamed Najim. Estimation of frequencies and damping factors by two-dimensional ESPRIT type methods. *IEEE Transactions on Signal Processing*, 49(1) :237–245, 2001.

[15] Roland Badeau, Bertrand David, and Gaël Richard. A new perturbation analysis for signal enumeration in rotational invariance techniques. *IEEE Transactions on Signal Processing*, 54(2) :450–458, 2006.

[16] Kefei Liu, Lei Huang, Hing Cheung, and Jieping Ye. Multidimensional folding for sinusoidal order selection. *Digital Signal Processing*, 48 :349–360, 2016.